JACS
JOURNAL OF THE AMERICAN CHEMICAL SOCIETY
Article
pubs.acs.org/JACS

π-Face Donation from the Aromatic N-Substituent of N-Heterocyclic Carbene Ligands to Metal and Its Role in Catalysis

Raffaele Credendino,[†,‡] Laura Falivene,[†] and Luigi Cavallo*[,†,‡]

[†]Dipartimento di Chimica e Biologia, Università di Salerno, Via Ponte don Melillo, I-84084 Fisciano (SA), Italy

[‡]King Abdullah University of Science and Technology (KAUST), Chemical and Life Sciences and Engineering, Kaust Catalysis Center, Thuwal 23955-6900, Saudi Arabia

Supporting Information

ABSTRACT: In this work, we calculate the redox potential in a series of Ir and Ru complexes bearing a N-heterocyclic carbene (NHC) ligand presenting different Y groups in the para position of the aromatic N-substituent. The calculated redox potentials excellently correlate with the experimental $\Delta E_{1/2}$ potentials, offering a handle to rationalize the experimental findings. Analysis of the HOMO of the complexes before oxidation suggests that electron-donating Y groups destabilize the metal centered HOMO. Energy decomposition of the metal−NHC interaction indicates that electron-donating Y groups reinforce this interaction in the oxidized complexes. Analysis of the electron density in the reduced and oxidized states of representative complexes indicates a clear donation from the C_{ipso} of the N-substituents to an empty d orbital on the metal. In case of the Ru complexes, this mechanism involves the Ru−alkylidene moiety. All of these results suggest that electron-donating Y groups render the aromatic N-substituent able to donate more density to electron-deficient metals through the C_{ipso} atom. This conclusion suggests that electron-donating Y groups could stabilize higher oxidation states during catalysis. To test this hypothesis, we investigated the effect of differently donating Y groups in model reactions of Ru-catalyzed olefin metathesis and Pd-catalyzed C−C cross-coupling. Consistent with the experimental results, calculations indicate an easier reaction pathway if the N-substituent of the NHC ligand presents an electron-donating Y group.

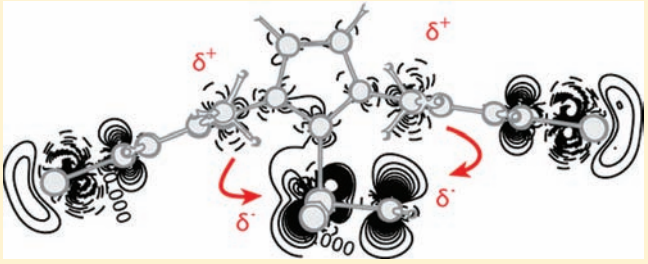

INTRODUCTION

If chemists should vote for the most relevant advances in catalysis over the last 20 years, N-heterocyclic carbenes (NHCs)[1−4] would certainly score in the top positions. Focusing on transition metal promoted catalysis, NHC ligands have been successfully tested in a number of rather different chemical transformations, such as Rh- and Ir-catalyzed hydrosilylation,[3,5] C−H activation[3,6,7] and hydrogenations,[8,9] Au-catalyzed cyclization of polyunsaturated substrates[10] and C−H activation of acetylenes,[11] Cu-catalyzed borylation reactions,[12,13] and finally in the Ni-catalyzed dehydrogenation of ammonia−borane to H_2.[14] However, the fields where the largest impact is foreseen are the Nobel reactions 2005 and 2010, which means Ru-catalyzed olefin metathesis[15,16] and Pd-catalyzed cross-coupling reactions.[3,17−19] Both of these reactions are extremely versatile and allow chemists to perform fundamental manipulations on the C−C and C=C bonds. NHC ligands have been tested in both of the above reactions and gave unusual or better reactivity in comparison with classical phosphines. Ru and Pd catalysts bearing NHC ligands are in the catalogue of basically all catalyst suppliers and have entered the world of industrial applications.

This practical interest for NHC as privileged ligands in transition metal promoted catalysis has spurred impressive research to understand the details of the M−NHC bond,[20−39] and the way this bonding influences catalytic behavior.[40,41] The most updated model of the M−NHC bond consists of a dominating σ-donation from the HOMO of the NHC ligand, centered on the carbene C atom, to empty d orbitals of the metal. This σ-bond is reinforced by donation from π orbitals on the NHC ligand to empty d orbitals of electron-deficient metals. However, NHC can also act as π-acid ligands, by accepting backdonation from filled d orbitals of electron-rich metals. The main characteristic of this bonding scheme is that the M−NHC interaction occurs via σ and π bonds between the metal and the carbene atom.

As is common in science, this scenario is being perturbed by new experiments. For example, in case of Ru-precatalysts for olefins metathesis based on NHC ligands presenting aromatic N-substituents, Fürstner observed that the short C−C distance between the benzylidene unit and the *N*-aryl rings of the NHC ligand would be consistent with a π-stacking interaction between the two aromatic rings.[42] Along a similar line, Plenio et al. demonstrated that the redox potential of several Ru, Pd, Ir, and Rh NHC-based complexes depends on the nature of the substituents at the para position of the *N*-xylyl rings.[43−47] This was found puzzling because communication through the σ-

Received: December 28, 2011
Published: April 23, 2012

   dx.doi.org/10.1021/ja212133j | J. Am. Chem. Soc. 2012, 134, 8127−8135

bonds is unlikely, seven bonds separate these substituents from the redox-active metal center, and communication through the π-orbitals is equally unlikely, as the aromatic ring of the N-substituent is orthogonal to the NHC ring.[46] This led the authors to conclude that communication between the NHC ligand and the metal center occurred through π-face donation.[43,45] A similar interaction was suggested to explain the conformation-dependent redox potential measured for a (diaminocarbene)Ir$(CO)_2$Cl complex.[48]

Intrigued by these experimental results, we decided to analyze the M−NHC interaction in complexes presenting groups with different electronic properties in the para position of the aryl N-substituent to provide a theoretical support to the experimental evidence that communication between the NHC ligand and the metal center can occur through π-face donation.[43,45] To tune the computational protocol, we first tested the chosen DFT tool to reproduce the experimental redox potential, $E_{1/2}$, of the Ir and Ru complexes shown in Chart 1. Systems **9**−**12** allow one to extend this tuning of the computational protocol to the prediction of the redox potential of complexes presenting different substitution at the alkoxy-alkylidene moiety.[49] The good agreement we found between calculated redox potential and experimental $\Delta E_{1/2}$ allowed us to perform a detailed analysis of the influence of the various substituents on the M−NHC bond. This knowledge is used to investigate the electronic property of the metal center in newly developed Ru-catalysts.[50−52] Finally, to test whether this interaction remains an academic curiosity or can influence catalysis, we investigated key structures along the reaction pathway of Ru-catalyzed olefins metathesis and Pd-catalyzed C−C cross-coupling reactions.

Chart 1. Systems Investigated in the Present Study

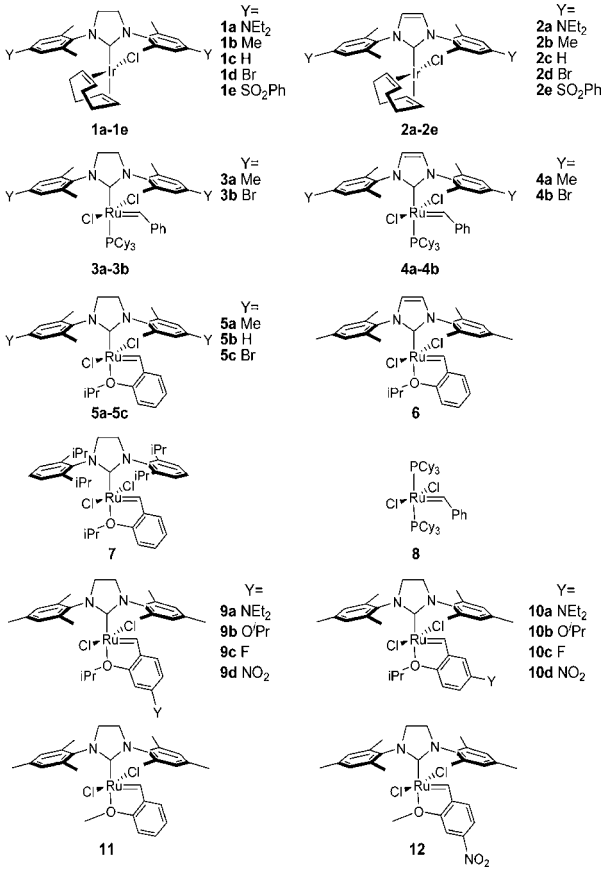

COMPUTATIONAL DETAILS

Geometry optimization of both the reduced and the oxidized complexes was performed at B3LYP[53−55] level with the Gaussian 09 package.[56] The electronic configuration of the molecular systems was described by a triple-ζ basis set for main group atoms (TZVP keyword in Gaussian 09),[57] while for transition metals we used the small core quasirelativistic SDD effective core potentials, with the associated triple-ζ valence basis set (SDD keyword in Gaussian 09).[58−60] The closed-shell neutral species were treated within a restricted formalism, whereas the open-shell cationic oxidized species were treated with an unrestricted formalism. All geometries were confirmed as minimum energy geometry through vibrational analysis.

The DFT redox potential E^{RedOx} was evaluated as indicated in eq 1:[61,62]

$$E^{\mathrm{RedOx}} = \frac{G^{\mathrm{Ox}} - G^{\mathrm{Red}}}{e^-} \qquad (1)$$

where E^{RedOx} is the DFT calculated one electron oxidation potential, G^{Ox} and G^{Red} are the free energies in solvent, of the oxidized and reduced systems, and e^- is electron charge. Solvent effects, CH_2Cl_2, have been estimated in single-point calculations on the gas-phase optimized structures, based on the polarizable continuum model PCM.[63−65]

To choose the most appropriate functional for the calculation of the redox potential of the systems reported in Chart 1, we tested the performance of a small series of functionals to reproduce the difference in the oxidation potential of prototype systems **1c** and **5b**, and of the experimentally used octamethylferrocene (**FC**) standard; see Table 1. The numbers reported in Table 1 clearly indicate that the simple GGA BP86[54,66] and PBEh[67,68] functionals perform reasonably well, with the difference in the oxidation potential of both **1c** and **5b** relative to **FC** in reasonable agreement with the experimental value. However, both of the GGA functionals tested wrongly predict the difference in the redox potential of **1c** and **5b**, with **5b** more easily oxidized than **1c**. Differently, the HGGA PBE0[69] and B3LYP[70] functionals underestimate severely the redox potential of both **1c** and **5b** versus **FC**, ruling out the accurate prediction of the redox potential by these functionals. The last generation HMGGA M06 functional,[71] instead, performs remarkably well, offering an almost perfect reproduction of the relative redox potential of **1c**, **5b**, and **FC**. For this reason, in the rest of this Article, we decided to report the redox potential in CH_2Cl_2 calculated with the M06 functional on the B3LYP geometries. Zero-point energies and thermal corrections at the B3LYP level were added to the M06 energies in solvent to achieve the best approximation to the free energies in solvent. However, we found that a slightly better correlation between the theoretical and the experimental redox potentials of the systems shown in Chart 1 is obtained with the simple M06 energies in solvent, $R^2 = 0.92$ and a mean unsigned error of 0.45 V, rather than by adding the B3LYP zero-point energies and thermal corrections to the in solvent M06 energies, $R^2 = 0.88$ and mean unsigned error of 0.53 V. For this reason, the redox potentials discussed below are calculated with the simple M06 energies in

Table 1. Relative Redox Potential, in volt, of the Selected Systems

	1c−FC	5b−FC	1c−5b
exp.	0.759	0.870	−0.111
BP86	0.798	0.743	0.055
PBEh	0.762	0.695	0.067
PBE0	0.194	0.359	−0.165
B3LYP	0.073	0.296	−0.223
M06	0.767	0.811	−0.044

dx.doi.org/10.1021/ja212133j | J. Am. Chem. Soc. 2012, 134, 8127−8135

solvent. All of the redox potentials reported in the following, indicated as ΔE^{redox}(DFT), are calculated relative to the calculated oxidation potential of **FC**.

The electron density difference maps were calculated using a common geometry for the (NHC)(Cl_2)Ru=CH_2 skeleton. Specifically, the geometry of the neutral **12b** (see later) is used in all of these calculations, with the geometry of **12a** and **12c** obtained by replacing the para H atoms of **12b** with the NMe_2 and Br groups from the optimized geometry of the neutral **12a** and **12c**. These geometries have been also used for the cationic species. This allowed one to obtain a perfect overlap of the Ru, NHC, and =CH_2 skeleton, which resulted in clean electron density difference maps. Our attempts to use the optimized geometries of the complexes introduced too much noise in the electron density difference maps, due to the marginal displacements of the atoms between the different structures.

In case of the Pd-catalyzed C−C cross-coupling and of the Ru-catalyzed olefins metathesis reactions, the BP86 functional in connection with a split-valence basis set (SVP keyword in Gaussian) on all of the atoms was used.[54,66,72] For both Pd and Ru, we used the small core quasirelativistic SDD electron core potential, with the associated triple-ζ valence basis set (SDD keyword in Gaussian 09).[58−60] Also in this case, solvent effects, CH_2Cl_2, have been estimated in single-point calculations on the gas-phase optimized structures, based on the polarizable continuum model PCM.[63−65] Finally, while this Article was under review, another worthy paper describing π-interaction between the NHC ligand and the Ru−alkylidene moiety was published.[73]

RESULTS AND DISCUSSION

The DFT calculated redox potentials for the systems of Chart 1 are plotted against the experimental $\Delta E_{1/2}$ in Figure 1. The data

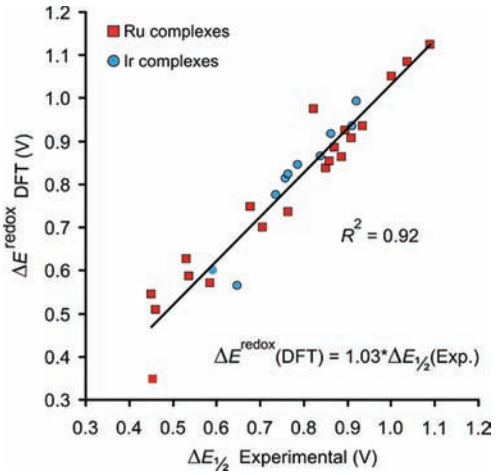

Figure 1. Plot of the DFT redox potentials versus the experimental $\Delta E_{1/2}$ for the Ir and Ru complexes shown in Chart 1.

reported in Figure 1 show that higher redox potentials correspond to NHC ligands presenting an electron-withdrawing group in the para position of the *N*-xylyl substituent, whereas a reduction in the redox potential is found when an electron-donating group is present in the para position of the *N*-xylyl substituent. From a quantitative point of view, the calculated redox potentials reproduce well the absolute experimental $\Delta E_{1/2}$ values, with a R^2 equal to 0.92. The mean unsigned error and the root-mean-square deviation between the calculated redox potentials and the experimental $\Delta E_{1/2}$ are equal to 45 and 58 mV, respectively, which gives an indication of the accuracy that can be expected when the protocol we developed is used to predict the $\Delta E_{1/2}$ of Ir or Ru complexes of the type shown in Chart 1. The very good agreement between the calculated redox potential and the experimental $\Delta E_{1/2}$ indicates that DFT calculations can be used to characterize the electronic properties of NHC ligands for which the experimental $\Delta E_{1/2}$ is not available, thus adding to the set of molecular descriptors used to classify NHC ligands in terms of steric and electronic properties.[26,74−77] Further, it validates the following analysis.

After the calculation protocol has been validated, we move to clarify if the Y group in the para position of the N-substituent influences the stability of the neutral species or of the cationic oxidized species. To this end, we examined if the $\Delta E_{1/2}$ correlates with the energy of the highest occupied molecular orbital (HOMO) of the neutral species, because the first ionization energy can be approximated with the HOMO in the framework of the Koopman's theorem.[78] This plot is reported in Figure 2. Inspection of the plot clearly shows an almost

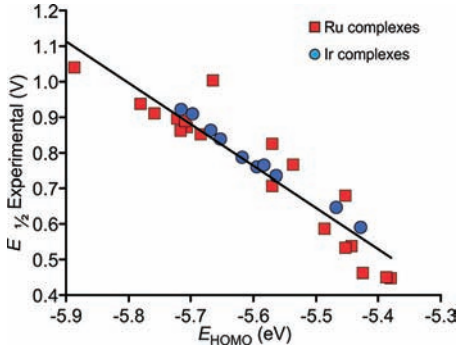

Figure 2. Plot of the experimental $\Delta E_{1/2}$ versus the DFT calculated HOMO energy for the systems of Chart 1.

linear and quantitative relationship between the energy of the HOMO, which is strongly centered on the Ir and the Ru atoms (for example, in the reference systems **1c** and **5b**, the HOMO is 78% on the Ir and 55% and 34% on the Ru and Cl atoms, respectively) and the experimental $\Delta E_{1/2}$ for both Ir and Ru complexes. This finding indicates that one effect of the Y group is to destabilize the neutral species by raising the energy of the HOMO.

Next, we examined selected M−NHC distances, because a change in the σ/π donicity from the NHC ring to the metal, possibly induced by the para Y groups, should influence the M−NHC bonding with a variation of the M−NHC distance. For the sake of simplicity, we focused this analysis on the Ir complexes **1b**−**1d** and **2b**−**2d**; the corresponding Ir−NHC distances are reported in Table 2. Analysis of the values reported in Table 2 indicates that the para Y groups do not influence the Ir−NHC distance both in the neutral and in the

Table 2. Key Geometric Parameters, Distances in Å, Angles in deg, in Selected Neutral and Cationic Ir-Complexes

	neutral			cationic		
	Ir−NHC	Ir−C_{para}	C_{carb}−N−C_{ipso}	Ir−NHC	Ir−C_{para}	C_{carb}−N−C_{ipso}
1b	2.073	5.514	127.7	2.060	5.327	126.0
1c	2.070	5.498	127.8	2.063	5.312	126.2
1d	2.068	5.467	127.5	2.063	5.281	125.9
2b	2.081	5.542	127.0	2.070	5.422	126.0
2c	2.079	5.518	127.0	2.071	5.378	125.8
2d	2.076	5.495	126.8	2.072	5.370	125.8

dx.doi.org/10.1021/ja212133j | J. Am. Chem. Soc. 2012, 134, 8127−8135

cationic species. For example, the Ir−NHC distance in the neutral system is reduced by only 0.005 Å on going from **1b** to **1d**, while in the corresponding cationic species the range spanned by the Ir−NHC distance is only 0.003 Å. Similar behavior is calculated for systems **2b−2d**, presenting an unsaturated NHC ligand. On the average, the Ir−NHC is 0.008 Å shorter in the cationic species, a clear consequence of the cationic nature of the complex after oxidation. This simple geometric analysis supports the idea that the Y groups cannot communicate with the metal center through the NHC ligand, and more specifically through the M−NHC bond.[46]

More rewarding, instead, is the analysis of the average Ir−C_{para} distance in complexes **1b−1d** and **2b−2d**; see again Table 2. In fact, the Ir−C_{para} distance shrinks by roughly 0.05 Å on going from Y = Me to Y = Br, both for the cationic and for the neutral systems. This change in the average Ir−C_{para} distance has already been evidenced by Plenio and co-workers, who noticed a longer average Ir−C_{para} distance in the X-ray structure of **1a**, 5.74 Å, than in that of **1c**, 5.27 Å.[46] For comparison, we calculated an average Ir−C_{para} distance slightly longer in **1a**, 5.54 Å, than in **1c**, 5.50 Å. This suggests that a longer Ir−C_{para} distance might be consistent with a more electron-donating Y group, because we found this effect consistently in the optimized geometries. Regarding the discrepancy between the calculated and the experimental values, this could be due to packing effects in the crystal structure (not considered in the calculations), or to the specific functional used. However, considering that the discrepancy between the experimental and the calculated values is around 4%, we believe this is an acceptable performance of the methodology, because this error is on a distance between two non interacting atoms. The small reduction of the Ir−C_{para} distance in the DFT geometry of **1a** and **1c** is consequence of a small reduction, roughly 0.2°, of the $C_{carbene}$−N−C_{ipso} angle, which basically pulls the aromatic ring of the N-substituents closer to the Ir atom in case of electron-withdrawing Y groups. Comparison of the neutral and cationic systems shows that the Ir−C_{para} distance is on average 0.16 Å shorter in the cationic species, while the $C_{carbene}$−N−C_{ipso} angle is on average 1.3° smaller in the cationic species. This indicates that after oxidation the N-aromatic substituents bend toward the metal considerably.

Next, we analyzed the energetics of the relaxation of **1b−1d** and **2b−2d** after oxidation. That is, we compared the energy of the oxidized species in the geometry of the reduced species to that of the oxidized species after geometry optimization. In case of **1b−1d** and **2b−2d**, the energy gain connected to a geometric relaxation after oxidation is 3.7 and 3.0 kcal/mol, respectively, with the Y group affecting this value by 0.1 kcal/mol only. This indicates that the main impact of the Y group is not in the geometry of the cationic species, but it is on the specific interaction between the NHC ligand and the metal. For this reason, we performed an energy decomposition analysis of the bonding between the NHC ligand and the Ir center in **1b−1d** and **2b−2d**; see Table 3. The total bond energy is decomposed as indicated in eq 2:

$$\mathrm{BDE} = E_{\mathrm{Snap}} + E_{\mathrm{Relax}} \qquad (2)$$

where BDE is the total bonding energy of the NHC ligand to the Ir center, E_{Snap} is the bond snapping energy, which is the energy required to separate rigidly the NHC and the Ir fragment in the geometry they have in the complex, and E_{Relax} is the relaxation energy, which is the energy gain obtained from relaxation of the NHC and Ir-fragments after separation.

Table 3. Gas-Phase Contributions of the Energy Decomposition Analysis, in kcal/mol, of the Ir−NHC Bond in 1b−1d and 2b−2d

	neutral			cationic		
	BDE	E_{Snap}	E_{Relax}	BDE	E_{Snap}	E_{Relax}
1b	60.6	73.9	−13.3	94.6	115.4	−20.8
1c	60.4	74.2	−13.8	92.5	113.0	−20.6
1d	59.9	73.6	−13.7	88.7	109.4	−20.7
2b	59.8	72.4	−12.6	92.2	112.6	−20.4
2c	59.6	72.6	−13.1	90.4	110.7	−20.3
2d	59.1	72.0	−12.8	86.5	106.7	−20.2

Analysis of the energetics reported in Table 3 shows that, in agreement with previous results,[79,80] the total bond dissociation energy, BDE, in the neutral **1b−1d** and **2b−2d** complexes is quite similar, with the BDEs in **1b−1d** roughly 1 kcal/mol greater than in **2b−2d**. This indicates that the saturated or unsaturated nature of the NHC skeleton has a minor impact on the BDE. Further, it also indicates that the nature of the Y group on the N-substituents has a minor impact on the BDE of the NHC ligand in the neutral species. Similar conclusions are obtained by comparing the E_{Snap} energies, which can be considered as a snapshot of the interaction between the NHC ligand and the Ir fragment in the geometry they have in the complex. Moving to the cationic species, the first clear result is the much higher BDEs, of course a consequence of a much stronger interaction between the charged metal fragment and the NHC ligand. Also, in case of the cationic systems, the difference in the BDE between systems **1b−1d** and **2b−2d** is marginal, although it slightly increases to ∼2 kcal/mol. Differently, in case of the cationic systems, the Y group has a clear influence on both the BDE and the E_{Snap}. Specifically, the NHC presenting an electron-donating Me group, **1b** and **2b**, shows a BDE and an E_{Snap} roughly 6 kcal/mol higher than those calculated for NHC presenting an electron-withdrawing Br group, **1d** and **2d**. This finding clearly indicates that electron-donating groups in the para position of the N-substituent reinforce the overall interaction between the NHC ligand and the metal in the cationic species.

To shed light on the mechanism through which the Y group in the para position of the N-substituents is able to destabilize the neutral species and to stabilize higher oxidation states, we analyzed the electron density in selected systems. For the sake of simplicity, and to highlight differences, we performed this analysis on the model systems shown in Chart 2. Models **13a−13c** are representative of an active species almost ubiquitous in Ru-catalyzed olefins metathesis, and thus this analysis starts to offer a vision of the influence of the Y group in the para position of the N-substituent during catalysis. Further, the unsaturated NHC ring allows one to work under C_S symmetry, with the symmetry plane coincident with the NHC plane.

Chart 2. Model Systems Used in the Electron Density Analysis

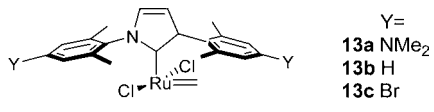

13a-13c

First, we compared the difference in the electron density, $\rho-\tilde{\rho}$, between the cationic and the neutral species of the

dx.doi.org/10.1021/ja212133j | J. Am. Chem. Soc. 2012, 134, 8127−8135

reference system **13b**. This plot indicates which is the redistribution of the electron density after oxidation. The electron density difference $\rho-\tilde{\rho}$ is plotted in the plane of the NHC ring as well as in the plane orthogonal to it, Figure 3a and b, respectively. Within this definition, red and blue lines (corresponding to positive and negative isocontour lines) indicate zones where the electron density is higher or lower in the cationic species, respectively.

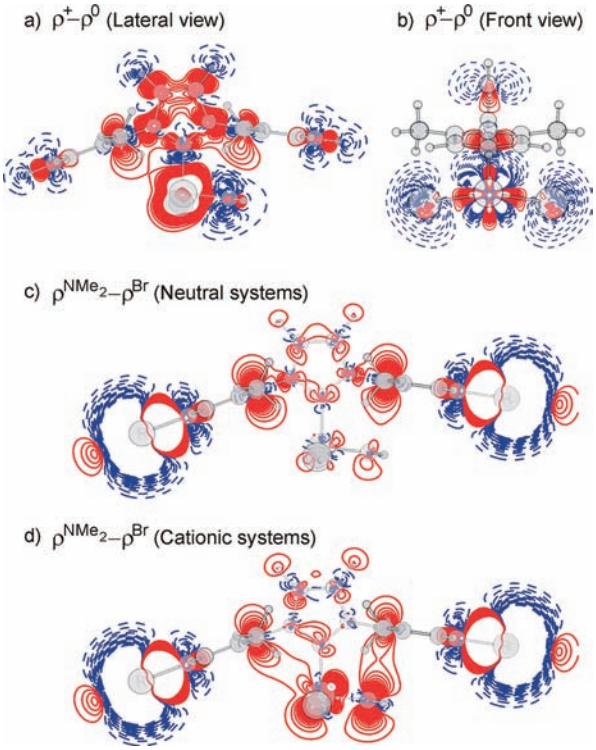

Figure 3. Plots of the electron density difference between the cationic and the neutral species of the Ru-system **13b**, $\rho^{+}-\rho^{0}$, parts a,b, and between the neutral and cationic species of the Ru-systems **13a** and **13c**, $\rho^{NMe2}-\rho^{Br}$, part c neutral systems, part d cationic systems. Red full and blue dashed lines indicate positive and negative isodensity lines, drawn between −0.01 and 0.01 au with a spacing of 0.0005 au.

Inspection of Figure 3a clearly shows the unexpected result that electron density at the metal, in the plane of the NHC ring, is higher in the cationic form rather than in the neutral form (see the red full lines around the Ru center in Figure 3a). Indeed, in agreement with the HOMO composition described above, the plot of Figure 3b clearly indicates that upon oxidation electron density is mainly removed from the metal center as well as from the chloride ligands (see the blue dashed lines around the Cl atoms in Figure 3b).

Focusing on a more detailed level, inspection of Figure 3a indicates that, to alleviate the electron deficiency at the metal center in the cationic species, electron density is accumulated on and transferred from the C_{ipso} atoms directly to the Ru center via a classical π to d donation, see left side of Figure 3a, as well as to the alkylidene C atom via a π (C_{ipso}) to π^* ($C_{alkylidene}$) donation, see right side of Figure 3a. The electron density donated from the C_{ipso} to the $C_{alkylidene}$ allows the alkylidene group to transfer electron density to the metal center, as indicated by the blue dashed lines around the alkylidene C atom in Figure 3a. This conclusion is consistent with the results reported in ref 73.

Within this scheme, the effect of the Y groups in the para position of the N-substituents becomes easily rationalized. Electron-donating groups reinforce electron density at the C_{ipso} of the NHC ligand, thus enhancing their ability to donate to both the metal center and the alkylidene group, whereas electron-withdrawing groups deplete electron density at the C_{ipso} of the NHC ligand, thus reducing their ability to donate electron density. Support to this analysis is given by a comparison of the electron density in the neutral and in the cationic systems presenting NMe_2 and Br Y groups, $\rho^{NMe2}-\rho^{Br}$, see Figure 3c,d. Within this definition, positive and negative isocontour lines (full and dashed lines in Figure 3c,d) indicate zones where the electron density is higher or lower in the species presenting an electron-donating NMe_2 group in the para position of the N-aryl ring. Inspection of Figure 3c shows that in the neutral species electron density at the metal as well as at the alkylidene group is substantially the same in **13a** and **13c**; the main difference (beside the area around the Y groups) is at the C_{ipso}. As in organic chemistry textbooks, electron density at the C_{ipso} is higher in the presence of the NMe_2 group. Differently, in the cationic species, the electron density in the plane of the NHC ring is quite higher around the metal center and around the alkylidene moiety in **13a**, while there is a reduction of excess density around the C_{ipso}. Further, in the cationic species **13a**, there is increased amount of electron density between the two C_{ipso} and the metal center on one side, and the alkylidene moiety on the other side.

As a final remark on structural effects, it is worthy to note that in the alkoxybenzylidene systems, the NHC is slightly more bent toward the empty coordination position trans to the Ru−alkylidene bond. This results in a shorter distance between the Ru atom and the C_{ipso} above the empty coordination position, relative to the corresponding PCy_3-based systems. For example, in the neutral **3a** and **5a**, this distance is 3.48 and 3.35 Å, respectively, while in the oxidized **3a** and **5a**, this distance is 3.56 and 3.30 Å, respectively. This suggests that in systems **3**−**4**, where the NHC can engage in a π-face interaction with the alkylidene C atom, the main mechanism of electron density transfer is through the alkylidene. Conversely, in systems **5**−**6**, where the rotated alkylidene cannot engage in a π-face interaction with the *N*-xylyl ring, the main mechanism is direct donation to the metal through the empty coordination position trans to the Ru−alkylidene bond. This dual mechanism could explain the similar perturbation that the same Y group has on the redox potential of systems **3**−**4** and **5**−**6**, although in the latter the Ru−alkylidene bond is rotated by 90°. Futther, it could explain the perturbation different Y groups have in systems **1**−**2**, where no alkylidene group is present, although the range spanned by the redox potential in the Ir complexes is reduced relative to the range spanned in the Ru complexes.[46]

In conclusion, all of the analyses we performed illuminate that the mechanism transmitting the properties of the groups on the para position of the N-substituents to the metal center operates via the aromatic system on the N-substituent, with the C_{ipso} atom acting as key messenger between the Y group and the metal center. In case of the Ru systems, this mechanism involves also the alkylidene group. Further, our analysis clearly indicated that the Y groups have a double effect. They destabilize the HOMO in the reduced species, and they reinforce the M−NHC interaction in the oxidized species.

To have a better insight on the role that the various groups around the Ru center have in determining the redox potential, we examined the systems shown in Chart 3. The calculated

dx.doi.org/10.1021/ja212133j | J. Am. Chem. Soc. 2012, 134, 8127−8135

Chart 3. Model Systems Used To Relate the Redox Potentials to Structural Features

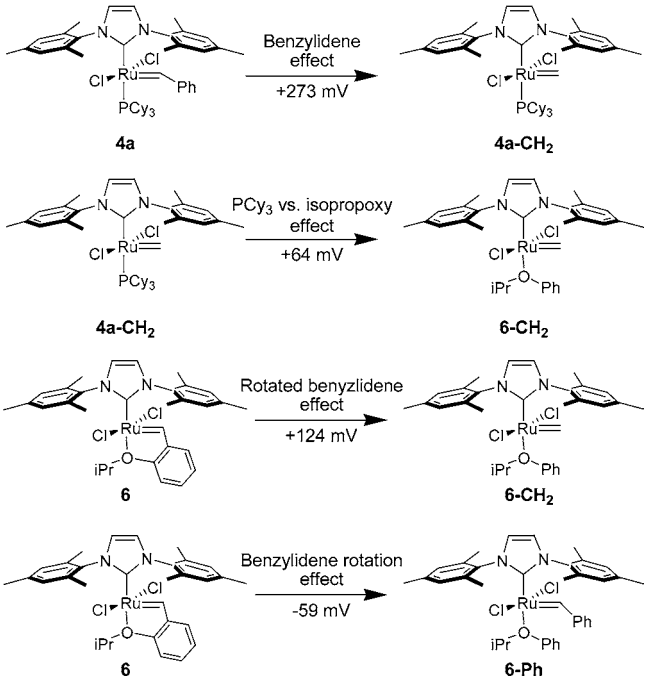

redox potential of **4a−CH$_2$** is 273 mV higher than that of **4a**, which indicates that the phenyl group of the benzylidene moiety, as expected, contributes remarkably to alleviate the electron deficiency at the metal atom after oxidation. On the other hand, the calculated redox potential of **6−CH$_2$** is only 64 mV higher than that calculated for **4a−CH$_2$**, which indicates that the PCy_3 is not that much better than the isopropoxy group in alleviating electron deficiency at the metal after oxidation. Instead, the calculated redox potential of **6−CH$_2$** is 124 mV higher than that of **6**. Comparison with the redox potential change calculated for **4a** → **4a−CH$_2$** highlights a reduced ability of the benzylidene moiety to transfer electron density to the metal when rotated in plane with the NHC ligand and when disengaged from π-face interaction with the above *N*-xylyl ring. Another estimate of the effect of the alkylidene rotation comes from the comparison of systems **6** and **6−Ph**, where the redox potential of the latter is 59 mV lower.

Having validated the computational protocol, and having clarified the mechanism through which the NHC ligand can impact the electron properties of the metal center, we wondered if this effect can have an impact on the performance of catalysts with potential large industrial applications. To this end, we considered the fundamental steps in the Ru-catalyzed olefins metathesis and in the Suzuki−Miyaura Pd-catalyzed C−C cross-coupling reaction. Starting with the Ru-catalyzed olefin metathesis, we first evaluated the redox potential of the two Ru-catalysts shown in Chart 4. These complexes represent innovative systems with remarkably improved performance in the synthesis of *Z*-olefins.[50−52] The innovation is in the presence of a caroboxylate ligand to replace one chloride ligand, and of a chelating Ru−C σ-bond involving one N-substituent of the NHC ligand, to replace the other chloride ligand. The peculiar geometry of **14** and **15** forces the mean plane of the NHC ligand to be rotated by roughly 22° and 90° away from the Ru−alkylidene bond, respectively. Consequently, this

Chart 4. Ru Systems Presenting a Chelating NHC Ligand Investigated in This Study

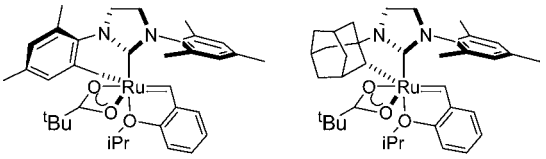

rotation pulls the mesityl group away from the Ru−alkylidene bond. Overall, these features make it difficult to easily place the metal center in **14** and **15** on a same electronic property scale with systems **3**−**12** of Chart 1. To this end, we calculated the redox potential of **14** and **15**. The calculated values, 0.602 and 0.615 V, respectively, characterize the metal center of these new catalysts as rather electron rich, because the calculated redox potential and the experimental $\Delta E_{1/2}$ of the chelating isopropoxy−alkylidene system **5a**, presenting an electron-donating Y = Me group, are equal to 0.838 and 0.850 V, respectively.

Next, we moved to investigate the effect of the Y group in the para position of the N-substituent in key structures along the reaction pathway of olefins metathesis. To this end, we evaluated the energy profile associated with PCy_3 dissociation, followed by ethene metathesis, with the systems shown in Chart 5, which means we evaluated the influence of the Y

Chart 5. Representative Systems Used To Investigate the Influence of the Y Group in Ru-Catalyzed Olefin Metathesis

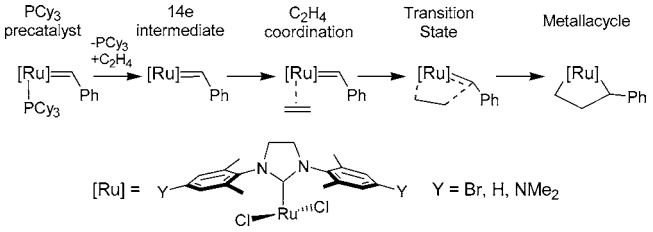

groups on olefin metathesis with a Ru−benzylidene complex in the framework of a completely dissociative mechanism, although there is growing evidence that an associative-interchange mechanism is very competitive.[49,81] However, competition between the various activation mechanism is out of the scope of this work. The energetics of the reaction shown in Chart 5 is reported in Table 4.

The numbers reported in Table 4 indicate that switching from an electron-withdrawing group such as Br, to an electron-donating group such as NMe_2, facilitates dissociation of the PCy_3 ligand, thus facilitating activation of the precatalyst, by roughly 1−2 kcal/mol. This energy difference is conserved at the level of the other species, including the transition state and

Table 4. Energy, in kcal/mol, of Ethylene Metathesis with the Ru-Systems Shown in Chart 5

	Y = NMe_2	Y = H	Y = Br
PCy_3 precatalyst	0.0	0.0	0.0
14e	14.0	14.6	15.5
C_2H_4 coordination	9.1	9.6	10.1
transition state	9.9	10.7	11.4
metallacycle	2.8	3.7	3.9

dx.doi.org/10.1021/ja212133j | J. Am. Chem. Soc. 2012, 134, 8127−8135

finally the metallacycle, where the Ru center is formally oxidized from Ru^{II} to Ru^{IV}. As a remark, it is worth noting that in the metallacycle the main transfer of electron density is direct donation from the *N*-xylyl ring to the metal, as in systems **1**−**2** and **5**−**6**, whereas in all other species the main transfer is mediated by the properly oriented alkylidene group, as in systems **3**−**4**.

This result correlates with the experimental evidence that in the ring-closing metathesis of diethyl diallylmalonate, the activity of Ru-catalysts with an isopropoxybenzylidene group is related to the electron richness of the respective Ru centers, with Y = NEt_2 > H ≫ Cl. This order of reactivity was also found in the ring-closing metathesis of diallyltosylamine.[46] These results are in line with the broad indication that activity of NHC-based Ru-catalysts in strictly related systems can be ranked according to the electron richness of the respective Ru centers[82] and provides a theoretical support to the experimentally based hypothesis that the nature of the aromatic "flaps" of the NHC ligands has a significant influence on the electron density at Ru center and on the catalytic properties of Grubbs-type complexes, and that this interaction occurs through π-face donation.[16,82]

On the other hand, it was also found that unsaturated and saturated NHC ligands with the same Y group presented rather different reactivity, despite the similar redox potential, and that the reactivity differences between catalysts with Y = NEt_2 and H were small as compared to the large differences in the redox potentials. This indicated that the redox potential cannot be used as a unique parameter to predict activity.[46]

Moving then to the C−C cross-coupling reaction, we evaluated the total energy change associated with the loading of two aryl units to the $(NHC)Pd^0$ center to form a transmetalated $(NHC)Pd^{II}(Ar)(Ar')$ (Ar = Ar′ = phenyl) intermediate, see eq 3, and on the following reductive elimination that leads to the coupled organic product.

$$(NHC)Pd + ArCl + Ar'B(OH)_2 + KOtBu \rightarrow (NHC)Pd(Ar)(Ar') + KCl + tBuOB(OH)_2 \quad (3)$$

This approach eliminates the specific way the two aryl moieties are loaded on the metal, which can be achieved in a rather large number of different approaches, allowing one to concentrate on the crucial reductive elimination step that will be present whatever reaction conditions are chosen to transmetallate the $(NHC)Pd^0$ intermediate. These steps were calculated for NHC presenting the H, NMe_2, and Br groups in the para position of the *N*-xylyl rings, and the corresponding energy plots are shown in Figure 4.

The first result is that loading the two aryl moieties on the Pd center is favored by 2.9 kcal/mol when the NHC with a NMe_2 group in the para position of the N-substituent is compared to a NHC presenting a Br group, the system with a H group being in the middle. The higher stability of the system presenting NMe_2 groups is maintained at the transition state for the reductive elimination cross-coupling step, in qualitative agreement with the hypothesis that electron-donating Y groups would stabilize species with the metal in a higher oxidation state. These results are indirectly consistent with the idea that more σ-donating ligands on Pd facilitate oxidative addition.[83−87] Further, it could be also possible that more stable Pd(II) species could be less prone to undergo deactivation reactions, resulting in overall higher activity.

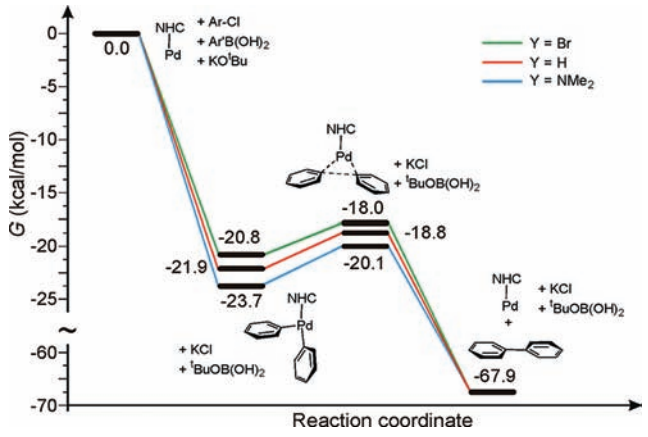

Figure 4. Energy profile for the Pd-catalyzed C−C cross-coupling reaction with selected NHC ligands.

CONCLUSIONS

Following experimental intuition, we have clarified and assessed a novel mode of interaction between NHC ligands bearing aromatic N-substituents and the metal. Rather than through the M−NHC σ/π bonds, this interaction operates "through space" via donation from the C_{ipso} atom of the N-substituent. Calculations have illuminated that this interaction can occur with two different mechanisms: (i) direct donation from the C_{ipso} of the N-aryl group to empty orbitals on the metal, such as in systems **1**−**2** and **5**−**6**; and (ii) by donation from the C_{ipso} of the N-aryl groups to additional groups bonded to the metal center, like the properly oriented alkylidene group in systems **3**−**4**, which act as transmitters of electron density from the C_{ipso} to the metal. Test calculations on model systems active in Pd-catalyzed cross-coupling reactions and in Ru-catalyzed olefins metathesis have evidenced how this interaction, consistently with experiments, can have an impact in catalysis, thus offering a handle for the rational tuning of the electronic properties of catalysts. As a final remark, it is worthy to note that the large distance between the groups in para of the N-substituents and the metal center allows one to modify the electronic properties of the system without influencing steric properties. Of course, a similar influence can be achieved with electron active groups in the ortho positions of the N-substituents, which would allow one to modify at the same time both steric and electronic properties.

ASSOCIATED CONTENT

Supporting Information

Calculated redox potentials, Cartesian coordinates and absolute energy of the discussed structures, and complete ref 56. This material is available free of charge via the Internet at http://pubs.acs.org.

AUTHOR INFORMATION

Corresponding Author

lcavallo@unisa.it; luigi.cavallo@kaust.edu.sa

Notes

The authors declare no competing financial interest.

ACKNOWLEDGMENTS

This project has been supported by the European Community (FP7 project CP-FP 211468-2 EUMET).

REFERENCES

(1) Arduengo, A. J.; Harlow, R. L.; Kline, M. *J. Am. Chem. Soc.* **1991**, *113*, 361.
(2) Glorius, F. *Top. Organomet. Chem* **2007**, *21*, 1.
(3) Diez-Gonzalez, S.; Marion, N.; Nolan, S. P. *Chem. Rev.* **2009**, *109*, 3612.
(4) *Heterocyclic Carbenes in Transition Metal Catalysis and Organocatalysis*; Cazin, C. S. J., Ed.; Springer: Dordecht, 2011; Vol. 32.
(5) Wolfgang, A. H.; Lukas, J. G.; Christian, K.; Georg, R. J. A. *Angew. Chem., Int. Ed. Engl.* **1996**, *35*, 2805.
(6) Danopoulos, A. A.; Pugh, D.; Wright, J. A. *Angew. Chem., Int. Ed.* **2008**, *47*, 9765.
(7) Hanasaka, F.; Tanabe, Y.; Fujita, K.-i.; Yamaguchi, R. *Organometallics* **2006**, *25*, 826.
(8) Lee, H. M.; Jiang, T.; Stevens, E. D.; Nolan, S. P. *J. Am. Chem. Soc.* **2001**, *20*, 1255.
(9) Powell, M. T.; Hou, D.-R.; Perry, M. C.; Cui, X.; Burgess, K. *J. Am. Chem. Soc.* **2001**, *123*, 8878.
(10) Marion, N.; Lemiere, G.; Correa, A.; Costabile, C.; Ramon, R. S.; Moreau, X.; de Frémont, P.; Dahmane, R.; Hours, A.; Lesage, D.; Tabet, J. C.; Goddard, J. P.; Gandon, V.; Cavallo, L.; Fensterbank, L.; Malaria, M.; Nolan, S. P. *Chem.-Eur. J.* **2009**, *15*, 3243.
(11) Fortman, G. C.; Poater, A.; Levell, J. W.; Gaillard, S.; Slawin, A. M. Z.; Samuel, I. D. W.; Cavallo, L.; Nolan, S. P. *Dalton Trans.* **2010**, *39*, 10382.
(12) Laitar, D. S.; Muller, P.; Sadighi, J. P. *J. Am. Chem. Soc.* **2005**, *127*, 17196.
(13) Kleeberg, C.; Dang, L.; Lin, Z.; Marder, T. B. *Angew. Chem., Int. Ed.* **2009**, *48*, 5350.
(14) Keaton, R. J.; Blacquiere, J. M.; Baker, R. T. *J. Am. Chem. Soc.* **2007**, *129*, 1844.
(15) Vougioukalakis, G. C.; Grubbs, R. H. *Chem. Rev.* **2009**, *110*, 1746.
(16) Samojłowicz, C.; Bieniek, M.; Grela, K. *Chem. Rev.* **2009**, *109*, 3708.
(17) Assen, E.; Kantchev, B.; O'Brien, C. J.; Organ, M. G. *Angew. Chem., Int. Ed.* **2007**, *46*, 2768.
(18) Marion, N.; Nolan, S. P. *Acc. Chem. Res.* **2008**, *41*, 1440.
(19) Würtz, S.; Glorius, F. *Acc. Chem. Res.* **2008**, *41*, 1523.
(20) Hu, X. L.; Castro-Rodriguez, I.; Olsen, K.; Meyer, K. *Organometallics* **2004**, *23*, 755.
(21) Frenking, G.; Fröhlich, N. *Chem. Rev.* **2000**, *100*, 717.
(22) Nemcsok, D.; Wichmann, K.; Frenking, G. *Organometallics* **2004**, *23*, 3640.
(23) Frenking, G.; Solà, M.; Vyboishchikov, S. F. *J. Organomet. Chem.* **2005**, *690*, 6178.
(24) Hillier, A. C.; Sommer, W. J.; Yong, B. S.; Petersen, J. L.; Cavallo, L.; Nolan, S. P. *Organometallics* **2003**, *22*, 4322.
(25) Scott, N. M.; Dorta, R.; Stevens, E. D.; Correa, A.; Cavallo, L.; Nolan, S. P. *J. Am. Chem. Soc.* **2005**, *127*, 3516.
(26) Kelly, R. A., III; Clavier, H.; Giudice, S.; Scott, N. M.; Stevens, E. D.; Bordner, J.; Samardjiev, I.; Hoff, C. D.; Cavallo, L.; Nolan, S. P. *Organometallics* **2008**, *27*, 202.
(27) Herrmann, W. A.; Runte, O.; Artus, G. *J. Organomet. Chem.* **1995**, *501*, C1.
(28) Schumann, H.; Gottfriedsen, J.; Glanz, M.; Dechert, S.; Demtschuk, J. *J. Organomet. Chem.* **2001**, *617*, 588.
(29) Niehues, M.; Erker, G.; Kehr, G.; Schwab, P.; Fröhlich, R.; Blacque, O.; Berke, H. *Organometallics* **2002**, *21*, 2905.
(30) Herrmann, W. A.; Öfele, K.; Elison, M.; Kuhn, F. E.; Roesky, P. W. *J. Organomet. Chem.* **1994**, *480*, C7.
(31) Nikiforov, G. B.; Roesky, H. W.; Jones, P. G.; Magull, J.; Ringe, A.; Oswald, R. B. *Inorg. Chem.* **2008**, *47*, 2171.
(32) Lee, M. T.; Hu, C. H. *Organometallics* **2004**, *23*, 976.
(33) Penka, E. F.; Schlaepfer, C. W.; Atanasov, M.; Albrecht, M.; Daul, C. *J. Organomet. Chem.* **2007**, *692*, 5709.
(34) Ray, L.; Shaikh, M. M.; Ghosh, P. *Dalton Trans.* **2007**, 4546.
(35) Boehme, C.; Frenking, G. *Organometallics* **1998**, *17*, 5801.
(36) Samantaray, M. K.; Pang, K.; Shaikh, M. M.; Ghosh, P. *Inorg. Chem.* **2008**, *47*, 4153.
(37) Garrison, J. C.; Simons, R. S.; Kofron, W. G.; Tessier, C. A.; Youngs, W. J. *Chem. Commun.* **2001**, 1780.
(38) Tulloch, A. A. D.; Danopoulos, A. A.; Kleinhenz, S.; Light, M. E.; Hursthouse, M. B.; Eastham, G. *Organometallics* **2001**, *20*, 2027.
(39) Hu, X. L.; Tang, Y. J.; Gantzel, P.; Meyer, K. *Organometallics* **2003**, *22*, 612.
(40) Tonner, R.; Heydenrych, G.; Frenking, G. *Chem. Asian J.* **2007**, *2*, 1555.
(41) Jacobsen, H.; Correa, A.; Poater, A.; Costabile, C.; Cavallo, L. *Coord. Chem. Rev.* **2009**, *253*, 687.
(42) Fürstner, A.; Ackermann, L.; Gabor, B.; Goddard, R.; Lehmann, C. W.; Mynott, R.; Stelzer, F.; Thiel, O. R. *Chem.-Eur. J.* **2001**, *7*, 3236.
(43) Süßner, M.; Plenio, H. *Chem. Commun.* **2005**, 5417.
(44) Süßner, M.; Plenio, H. *Angew. Chem., Int. Ed.* **2005**, *44*, 6885.
(45) Leuthäußer, S.; Schwarz, D.; Plenio, H. *Chem.-Eur. J.* **2007**, *14*, 7195.
(46) Leuthäußer, S.; Schmidts, V.; Thiele, C. M.; Plenio, H. *Chem.-Eur. J.* **2008**, *14*, 5465.
(47) Wolf, S.; Plenio, H. *J. Organomet. Chem.* **2009**, *694*, 1487.
(48) Collins, M. S.; Rosen, E. L.; Lynch, V. M.; Bielawski, C. W. *Organometallics* **2010**, *29*, 3047.
(49) Thiel, V.; Hendann, M.; Wannowius, K.-J.; Plenio, H. *J. Am. Chem. Soc.* **2011**, *134*, 1104.
(50) Keitz, B. K.; Endo, K.; Patel, P. R.; Herbert, M. B.; Grubbs, R. H. *J. Am. Chem. Soc.* **2012**, *134*, 693.
(51) Keitz, B. K.; Endo, K.; Herbert, M. B.; Grubbs, R. H. *J. Am. Chem. Soc.* **2011**, *133*, 9686.
(52) Endo, K.; Grubbs, R. H. *J. Am. Chem. Soc.* **2011**, *133*, 8525.
(53) Lee, C.; Yang, W.; Parr, R. G. *Phys. Rev. B* **1988**, *37*, 785.
(54) Becke, A. D. *Phys. Rev. A* **1988**, *38*, 3098.
(55) Becke, A. D. *J. Chem. Phys.* **1993**, *98*, 5648.
(56) Frisch, M. J.; et al. *Gaussian 09*; Gaussian, Inc.: Wallingford, CT, 2009.
(57) Schaefer, A.; Huber, C.; Ahlrichs, R. *J. Chem. Phys.* **1994**, *100*, 5829.
(58) Leininger, T.; Nicklass, A.; Stoll, H.; Dolg, M.; Schwerdtfeger, P. *J. Chem. Phys.* **1996**, *105*, 1052.
(59) Kuechle, W.; Dolg, M.; Stoll, H.; Preuss, H. *J. Chem. Phys.* **1994**, *100*, 7535.
(60) Haeusermann, U.; Dolg, M.; Stoll, H.; Preuss, H. *Mol. Phys.* **1993**, *78*, 1211.
(61) Shimodaira, Y.; Miura, T.; Kudo, A.; Kobayashi, H. *J. Chem. Theory Comput.* **2007**, *3*, 789.
(62) Roy, L. E.; Jakubikova, E.; Guthrie, M. G.; Batista, E. R. *J. Phys. Chem. A* **2009**, *113*, 6745.
(63) Miertus, S.; Scrocco, E.; Tomasi, J. *J. Chem. Phys.* **1981**, *55*, 117.
(64) Tomasi, J.; Persico, M. *Chem. Rev.* **1994**, *94*, 2027.
(65) Cossi, M.; Barone, V.; Cammi, R.; Tomasi, J. *Chem. Phys. Lett.* **1996**, *255*, 327.
(66) Perdew, J. P. *Phys. Rev. B* **1986**, *33*, 8822.
(67) Ernzerhof, M.; Perdew, J. P. *J. Chem. Phys.* **1998**, *109*, 3313.
(68) Perdew, J. P.; Burke, K.; Ernzerhof, M. *Phys. Rev. Lett.* **1996**, *77*, 3865.
(69) Adamo, C.; Barone, V. *J. Chem. Phys.* **1999**, *110*, 6158.
(70) Stephens, P. J.; Devlin, F. J.; Chabalowski, C. F.; Frisch, M. J. *J. Phys. Chem.* **1994**, *98*, 11623.
(71) Zhao, Y.; Truhlar, D. *Theor. Chem. Acc.* **2008**, *120*, 215.
(72) Perdew, J. P. *Phys. Rev. B* **1986**, *34*, 7406.
(73) Fernández, I.; Lugan, N.; Lavigne, G. *Organometallics* **2012**, *31*, 1155.
(74) Poater, A.; Cosenza, B.; Correa, A.; Giudice, S.; Ragone, F.; Scarano, V.; Cavallo, L. *Eur. J. Inorg. Chem.* **2009**, 1759.
(75) Occhipinti, G.; Bjorsvik, H. R.; Jensen, V. R. *J. Am. Chem. Soc.* **2006**, *128*, 6952.
(76) Mathew, J.; Suresh, C. H. *Organometallics* **2011**, *30*, 3106.
(77) Fey, N. *Dalton Trans.* **2010**, *39*, 296.
(78) Koopmans, T. *Physica* **1934**, *1*, 104.

(79) Fantasia, S.; Petersen, J. L.; Jacobsen, H.; Cavallo, L.; Nolan, S. P. *Organometallics* **2007**, *26*, 5880.
(80) Jacobsen, H.; Correa, A.; Costabile, C.; Cavallo, L. *J. Organomet. Chem.* **2006**, *691*, 4350.
(81) Vorfalt, T.; Wannowius, K. J.; Plenio, H. *Angew. Chem., Int. Ed.* **2010**, *49*, 5533.
(82) Dias, E. L.; Nguyen, S. T.; Grubbs, R. H. *J. Am. Chem. Soc.* **1997**, *119*, 3887.
(83) Guram, A. S.; Wang, X.; Bunel, E. E.; Faul, M. M.; Larsen, R. D.; Martinelli, M. J. *J. Org. Chem.* **2007**, *72*, 5104.
(84) Schilz, M.; Plenio, H. *J. Org. Chem.* **2012**, *77*, 2798.
(85) Shekhar, S.; Ryberg, P.; Hartwig, J. F.; Mathew, J. S.; Blackmond, D. G.; Strieter, E. R.; Buchwald, S. L. *J. Am. Chem. Soc.* **2006**, *128*, 3584.
(86) Hills, I. D.; Netherton, M. R.; Fu, G. C. *Angew. Chem., Int. Ed.* **2003**, *42*, 5749.
(87) Nasielski, J.; Hadei, N.; Achonduh, G.; Kantchev, E. A. B.; O'Brien, C. J.; Lough, A.; Organ, M. G. *Chem.-Eur. J.* **2010**, *16*, 10844.